Algal Research 68 (2022) 102899

Contents lists available at ScienceDirect

Algal Research

journal homepage: www.elsevier.com/locate/algal

Elucidating the role of nanoparticles on photosynthetic biogas upgrading: Influence of biogas type, nanoparticle concentration and light source

Laura Vargas-Estrada [a,b,c], Edwin G. Hoyos [a,b], P.J. Sebastian [c], Raúl Muñoz [a,b,*]

[a] Institute of Sustainable Processes, University of Valladolid, C/Dr. Mergelina s/n., Valladolid 47011, Spain
[b] Department of Chemical Engineering and Environmental Technology, University of Valladolid, C/Dr. Mergelina s/n., Valladolid 47011, Spain
[c] Instituto de Energías Renovables, Universidad Nacional Autónoma de México, Temixco, Morelos CP. 62580, Mexico

ARTICLE INFO

Keywords:
Biogas upgrading
Biomass productivity
Microalgae
Nanoparticles
Optimization
UV exposure

ABSTRACT

Three different nanoparticles, namely Fe_2O_3, carbon coated zero valent iron (CACOI) and SiO_2, were added to a mixed microalgae culture in order to improve photosynthetic biogas upgrading. Fe_2O_3 and CACOI nanoparticles at 10 mg/L supported higher CO_2 consumptions compared to their respective controls. The addition of Fe_2O_3 nanoparticles at 70 mg/L resulted in a 38 % enhanced biomass productivity, and 20 % higher CO_2 consumption but delayed exponential growth. The CACOI nanoparticles at 70 mg/L resulted in a shorter lag phase, enhanced CO_2 consumption by 13 %, and carbohydrate content enhancement by 64 %, while the addition of SiO_2 nanoparticles at this concentration induced an enhanced lipid and carbohydrates production by 47 % and 68 %, respectively. Interestingly, UV light exposure reduced the beneficial effects of nanoparticles, although CACOI nanoparticles still supported a shorter lag phase and higher carbohydrates production at 70 mg/L. In brief, CACOI nanoparticles hold an untapped potential to promote the metabolism of microalgae during photosynthetic biogas upgrading.

1. Introduction

Biogas has become a relevant renewable energy source with the potential to substitute natural gas in the context of the World's Ecological Transition. Biogas is typically produced via anaerobic digestion of organic matter and its composition varies depending on the redox state of the substrates, environmental and operational conditions in the digesters. This green gas vector is mainly composed of CH_4 (45–75 %), CO_2 (25–55 %) and H_2S (0.005–2 %) [1]. In this context, the removal of contaminants such as CO_2 and H_2S is mandatory prior to its use as a vehicle fuel or to its injection to the natural gas grid [2]. Today, several physical and chemical methods are commercially available for biogas upgrading, including membrane separation, cryogenic separation, pressure swing adsorption, water scrubbing, organic solvent scrubbing, and chemical absorption [3]. The high operating costs and environmental impacts of these physical/chemical technologies have triggered research in biological methods such hydrogenotrophic and photosynthetic biogas upgrading.

Photosynthetic biogas upgrading in microalgae-bacteria photobioreactors has been validated at pilot and demo-scale, and widely reported to be an economically and environmentally friendly option to upgrade biogas into biomethane coupled to nutrient recovery from the liquid fraction of digestates [4]. Despite algal-bacterial photobioreactors interconnected to external biogas absorption columns have reached CO_2 removals of up to 98.6 % at pilot [5] and demo scale [4], there are still some challenges that need to be addressed to maintain a robust biogas upgrading performance. Recently, Bose et al. [6] compared seven different factors affecting the bubble column performance in photosynthetic biogas upgrading. The main process limitations identified to date are i) the low CO_2 mass transfer to the culture medium, ii) the high sensitivity of biomethane quality to variations in the gas and liquid flow rates and pH, and iii) the diurnal and seasonal variability of environmental parameters influencing photosynthetic activity [7]. Indeed, this process requires the development of innovative operational strategies to

Abbreviations: BA, biogas A; BB, biogas B; BET, Brunauer–Emmett–Teller; BJH, Barrett, Joyner & Halenda; CACOI, carbon coated zero valent iron; CH_4, methane; CO_2, carbon dioxide; EDS, energy dispersive spectroscopy; Fe_2O_3, iron (III) oxide; H_2S, hydrogen sulfide; IUPAC, International Union of Pure and Applied Chemistry; LED, light-emitting diode; NPs, nanoparticles; OD_{750}, optical density at 750 nm; Px, biomass productivity; ROS, reactive oxygen species; RuBisCO, Ribulose-1,5-bisphosphate carboxylase-oxygenase; SEM, Scanning Electron Microscopy; SiO_2, silicon dioxide; TSS, total suspended solids.

* Corresponding author at: Institute of Sustainable Processes, University of Valladolid, C/Dr. Mergelina s/n., Valladolid 47011, Spain.
E-mail address: mutora@iq.uva.es (R. Muñoz).

https://doi.org/10.1016/j.algal.2022.102899
Received 26 September 2022; Received in revised form 24 October 2022; Accepted 9 November 2022
Available online 15 November 2022

Table 1
Effect of nanoparticles on microalgae growth. PAN: polyacrylonitrile; DMF: dimethylformamide (DMF); NFs: nanofibers.

NP	Strain	CO_2 source	Effect	Reference
Fe_2O_3	*Chlorella vulgaris*		At concentrations of 50 and 100 mg/L biomass growth was reduced by 41.2 % and 83.7 % whereas total lipid contents increased by 39.7 % and 25.5 % respectively.	[17]
g-C_3N_4	*Scenedesmus* sp.		Improved biomass and lipid accumulation	[18]
PAN/DMF NFs with 4 % (w/v) Fe_2O_3 NPs	*Chlorella fusca* LEB 111	15 % v/v CO_2 gas	Assays with 0.3 g/L nanofibers supported 10.9 % greater lipid production than the assays without nanofiber	[13]
SiC	*Scenedesmus* sp.		Improved biomass and lipid accumulation	[18]
TiC			Inhibitory effect	
TiO_2				
TiO_2	*Dunaliella tertiolecta*		No evidence of NPs mediated inhibition of the growth or pigment content at concentrations up to 10 mg/L	[19]
ZnO	*Dunaliella tertiolecta*		Growth was reduced at concentration of 1 mg/L	[20]
ZnO	*Skeletonema costatum*		Growth was inhibited at 0.5 mg/L	[21]
ZVI	*Arthrospira maxima*		Growth and lipid accumulation were stimulated at concentrations between 1.7 and 5.1 mg/L	[16]
	Desmodesmus subspicatus *Dunaliella salina* *Nannochloropsis limnetica* *Parachlorella kessleri* *Raphidocelis subcapitata* *Trachydiscus minutus*		Growth and lipid accumulation were stimulated at a concentration of 5.1 mg/L	
ZVI	*Isochrysis galbana*		Preference to nanoparticles over EDTA-Fe	[15]
	Pavlova lutheri		Increase in lipid content	
	Tetraselmis suecica		Increased total cellular lipid content	

enhance CO_2 absorption and fixation.

During the past years, the use of nanomaterials in environmental applications is gaining attention due to their unique physicochemical properties such as size, morphology, high reactivity, chemical stabilization, high surface area-to-volume ratio, abundant active sites and high adsorption capacity [8]. Indeed, nanomaterials and nanoparticles can play a key role in CO_2 capture technologies, biogas production and biogas upgrading processes [9]. To date, many solid adsorbents, mainly porous materials, have been effectively used to remove CO_2 from biogas, such as activated carbons and metal oxides [10]. Moreover, it is kwon that the use of metal oxide NPs mediates the formation of carbonates, bicarbonates and carboxylates when CO_2 interacts with the NPs surfaces [11]. In this context, the addition of nanoporous materials to microalgae cultures devoted to biogas upgrading can create a symbiosis where the materials adsorb CO_2 to form carbonates and bicarbonate species that can be further fixed via photosynthesis by microalgae. This would result in enhancements in biomass production and in the performance of biogas purification. In addition, it has been recently demonstrated that the supplementation of graphene oxide quantum dots under UV-light exposure stimulated the CO_2 capture and lipid production in *Chlorella pyrenoidosa* [12]. Thus, NPs can be also used as a strategy to scavenge the damage of solar UV radiation to microalgae.

The addition of metal oxide NPs to microalgae culture is still a controversial topic, since NPs can be toxic to some microalgae species or stimulate their growth and lipid production (Table 1). Even if there is very little information on how the NPs addition to microalgae culture can improve the CO_2 adsorption, the reported studies present promising results [13]. In this way, the physico-chemical properties of the NPs can represent an advantage to improve CO_2 adsorption since they can act as electron donors/acceptors and light conversion aids, or form carbonates when CO_2 interacts with their surface, among others. Jeon et al. [14] reported that SiO_2 NPs enhanced the gas-liquid mass transfer rate of CO_2 in *C. vulgaris* cultures, resulting in an enhanced growth and lipid production. Similarly, the use of polymeric nanofibers containing Fe_2O_3 NPs has been reported as a promising technique to enhance CO_2 fixation of *Chlorella fusca* LEB 111 cultures [13]. On the other hand, the addition of zero-valent iron NPs have proved to have beneficial effects on microalgae species like *Pavlova lutheri, Isochrysis galbana, Tetraselmis suecica* [15], *Desmodesmus subspicatus, Dunaliella salina, Parachlorella kessleri* and *Trachydiscus minutus* [16]. However, to the best of our knowledge, little is known about the effect of carbon NPs on microalgae culture. The literature on the effect of carbon-coated zero-valent iron NPs on microalgae and the number studies devoted to investigate the potential of NPs during photosynthetic biogas upgrading is scarce.

This study aimed at assessing the effect of two metal oxides NPs (Fe_2O_3 and SiO_2) and one magnetic NP (carbon coated zero-valent iron) on microalgae growth and photosynthetic biogas upgrading efficiency at laboratory scale in batch enclosed photobioreactors. Additionally, the influence of NPs concentration and light source (visible versus visible + UV) on the parameters above mentioned were also investigated.

2. Materials and methods

2.1. Nanoparticles and stock solutions

Three different metal nanoparticles were investigated. Fe_2O_3 NPs were synthesized according to [22], while SiO_2 nanopowder was purchased from Sigma Aldrich. The CACOI nanoparticles were kindly donated by CALPECH. Fresh stock solutions of 200 mg/L of each nanoparticle were prepared in microalgae mineral medium, and sonicated for one hour to prevent nanoparticle agglomeration and facilitate the addition of the NPs to the microalgae culture. To determine the surface area, pore volume and average pore diameter of the NPs herein used, a nitrogen physisorption analysis was conducted in an ASAP 2050 (Micromeritics, USA) at 77 K. The specific surface area and pore characteristics were determined by the BET method and BJH equation. Scanning electron microscopy (SEM) (JEOL JSM-6490LV) and energy-dispersive spectroscopy (EDS) (EDX-700/800, Hitachi, Japan) were carried out to determine the surface morphology and elemental composition of the target NPs.

2.2. Microalgae culture and biogas

The microalgae culture used in our study consisted of a consortium of microalgae and cyanobacteria composed of *Chlorella* sp. (91.30 %), *Nitzschia* sp. (7.56 %) and *Pseudanabaena* sp. (1.16 %) (percentages expressed in number of cells). The consortium was obtained from an outdoors 180 L pilot experimental plant treating real biogas and digestate from a 100 L sewage sludge digester located at the Institute of Sustainable Processes (Valladolid, Spain). The detailed description of

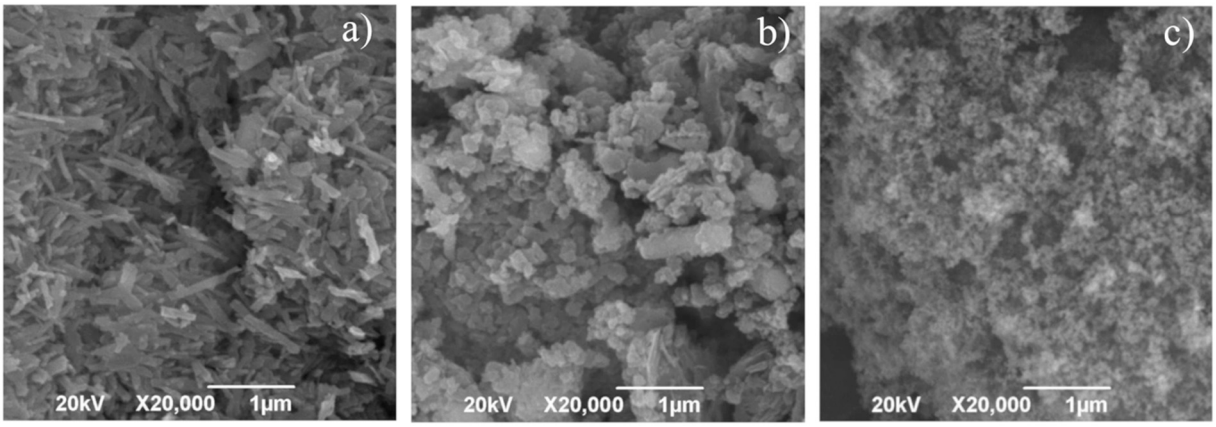

Fig. 1. Scanning Electron Microscope micrographs of a) Fe_2O_3, b) CACOI; carbon coated zero valent iron, and c) SiO_2 nanoparticles.

the pilot plant can be found elsewhere [23,24]. To elucidate the effect of NPs on photosynthetic biogas upgrading, two different synthetic biogas mixtures were used: Biogas A composed of CO_2 (30 %) and CH_4 (70 %) (Carburos Metalicos; Spain), and Biogas B composed of CO_2 (29.5 %), H_2S (0.5 %) and CH_4 (70 %) (Abello Linde; Spain).

2.3. Experimental set-up

Batch assays to quantitatively evaluate the effect of the different nanoparticles at different concentrations and under different light sources on biogas upgrading by microalgae were conducted in 1.2 L glass bottles. The bottles were prepared with 1 L of synthetic biogas headspace and 0.2 L of working volume, which was composed of mineral salt medium rich in carbonates as described elsewhere [25] and the corresponding nanoparticle concentration. The bottles were closed with butyl septa and plastic caps, flushed with helium for 5 min and, subsequently, the corresponding synthetic biogas was flushed for 5 min using inlet and outlet needles to replace the helium headspace. After one hour of stabilization, the bottles were inoculated with the mixed algal culture at an initial concentration of 200 mg/L of TSS. Then, the bottles were incubated at 25 °C under continuous magnetic stirring (300 rpm) to avoid microalgae sedimentation. Light intensity of 900 μE/m^2s was continuously provided by visible LED lights.

This study was divided in three tests series. In the tests series I, four operational conditions were evaluated for each nanoparticle: 1) Microalgae biomass and synthetic biogas A; 2) Microalgae biomass with 10 mg/L of nanoparticles and biogas A; 3) Microalgae biomass and synthetic biogas B; 4) Microalgae biomass with 10 mg/L of nanoparticles and biogas B. Each condition was run in triplicate. In tests series II, the influence of different concentrations (20, 40, and 70 mg/L) of each nanoparticle was assessed under biogas A headspace, 25 °C, magnetic stirring (300 rpm) and visible light 900 μE/m^2s. A control containing only algal biomass and biogas A was conducted. Each condition was run in triplicate. In test series III, the influence of different concentrations (20, 40, and 70 mg/L) of each nanoparticle was assessed under biogas A headspace, 25 °C, magnetic stirring (300 rpm) and visible light 900 μE/m^2s + UV light (λ 315–350 nm, 10 W/m^2). The UV light exposure was added to simulate real solar radiation. A control containing only algal biomass and biogas A was conducted. Each condition was run in triplicate.

2.4. Analytical procedures

The biogas composition in the headspace of the bottles was determined two times per day by gas chromatography-TCD (Bruker) to quantify the gas concentration of CH_4, CO_2, H_2S and O_2 in the headspace according to [26]. Microalgae growth was daily determined by optical density at 750 nm using a Shimadzu spectrophotometer (Japan), microalgae samples were daily taken and properly diluted to obtain an absorbance under 1, then the obtained absorbance was multiplied by the dilution factor. The initial CO_2 and O_2 content in the headspace along with the OD_{750} were normalized and are presented as cumulative values. pH was determined at the beginning and at the end of the experiment (SensION™ + PH3 pHmeter, HACH, Spain). TSS concentrations were determined according to standard methods [27]. The biomass obtained from test series II and II was harvested (10,000 rpm, 4 °C) and freeze-dried for further macromolecular characterization. The carbohydrate content was determined according to [28], while the lipid content was determined gravimetrically following biomass extraction with chloroform:methanol (2:1 v/v) as described elsewhere [29].

Table 2
Chemical composition of the different nanoparticles used. The values represent the atomic percentage. CACOI: carbon coated zero valent iron.

Element	Fe_2O_3	CACOI	SiO_2
Si (%)			19.70
O (%)	59.20	12.90	80.30
Na (%)	3.44		
Fe (%)	37.40	1.74	
C (%)		85.10	
P (%)		0.09	
K (%)		0.23	
Ca (%)		0.03	

2.5. Statistical analysis

The results are presented as mean values ± standard deviation. An analysis of variance (ANOVA) followed by Tuckey's test considering $\alpha = 0.05$ was performed to assess the influence of nanoparticles on microalgae growth.

3. Results and discussion

3.1. Nanoparticle characterization

The SEM micrographs show the morphology of the three NPs used in this study (Fig. 1). The Fe_2O_3 NPs presented a nanorod morphology, which has been previously reported to exhibit a high specific surface area and better electrochemical and magnetic properties compared to other Fe_2O_3 morphologies [30]. The CACOI NPs were characterized by agglomerated NPs in accordance with [31]. Finally, the SiO_2 NPs presented the smallest particle size among the three NPs tested. Moreover, the chemical composition of each NPs is presented in Table 2. The presence of Na in the Fe_2O_3 NPs was attributed to trace levels of the

Table 3
BET surface area, pore volume and average pore diameter of the nanoparticles used in this study. BET: Brunauer-Emmett-Teller; CACOI: carbon coated zero valent iron.

Nanoparticles	BET surface area (m^2/g)	Pore volume (cm^3/g)	Average pore diameter (nm)
Fe_2O_3	32.10	0.38	47.50
CACOI	27.30	0.28	41.50
SiO_2	981	6.97	28.40

catalyst used for their synthesis. Interestingly, the CACOI NPs exhibited low levels of essential minerals for microalgae growth, which could serve as nutrients and promote microalgae growth.

Furthermore, the BET surface area, pore volume and average pore diameter of the target NPs are shown in Table 3. The three NPs herein used presented pore diameters <50 nm, and according to the IUPAC classification, the three NPs represent mesoporous materials. In this context, the NPs can serve as gas adsorbents and promote a higher CO_2 biofixation. It is known that Fe_2O_3 NPs represent an effective adsorbent of CO_2 [32], Hakim et al. [33] reported that the CO_2 adsorption capacity of Fe_2O_3 increased up to four times when the particle size decreased from 160.5 nm (bulk form) to 24.5–56 nm. In our particular study, the

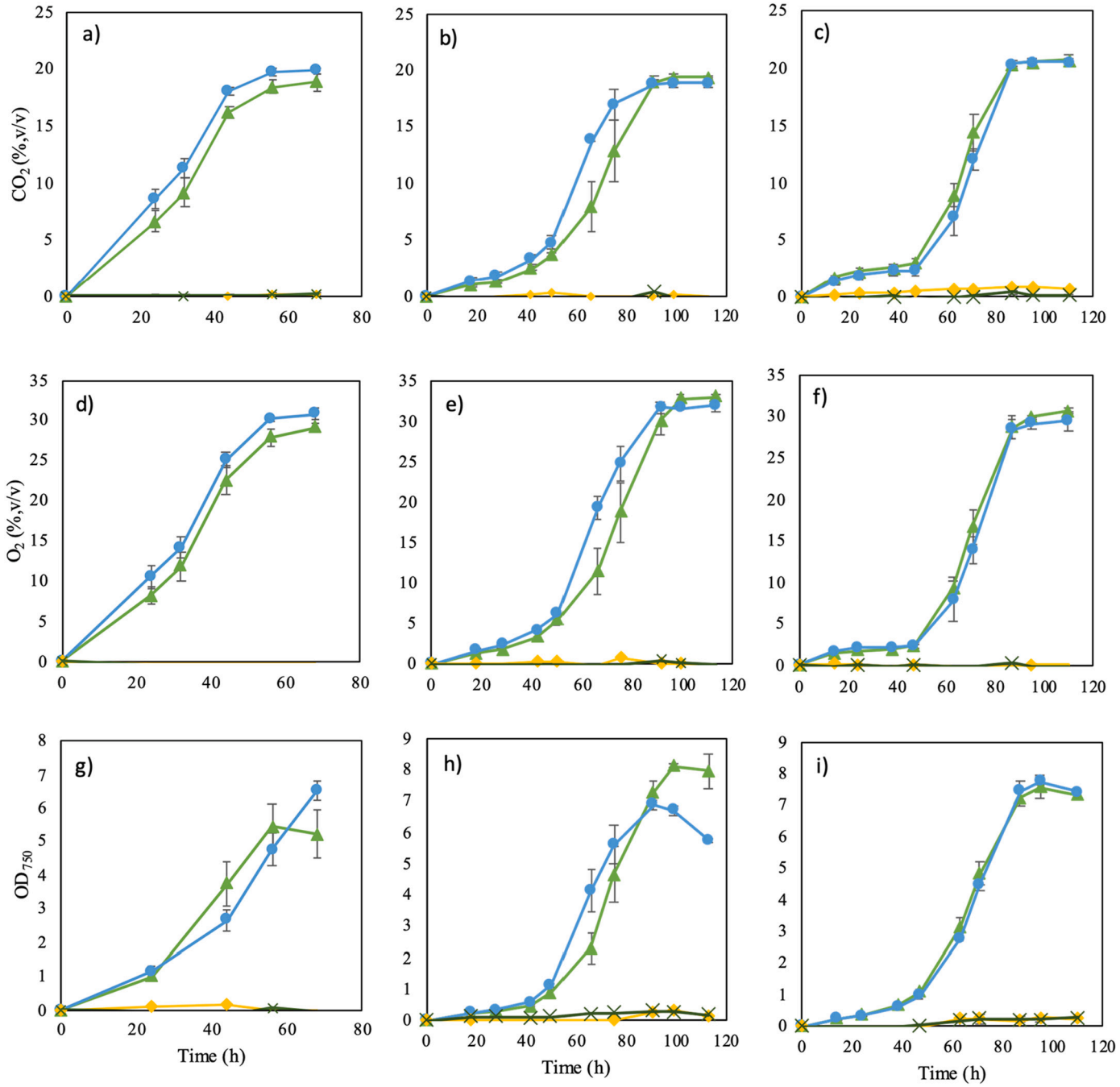

Fig. 2. Time course of the cumulative CO_2 consumption in the assays supplied with a) Fe_2O_3 NPs, b) CACOI NPs, c) SiO_2 NPs; cumulative O_2 production in the assays supplemented with d) Fe_2O_3 NPs, e) CACOI NPs, f) SiO_2 NPs; and culture absorbance of the algal consortium supplied with g) Fe_2O_3 NPs, h) CACOI NPs, i) SiO_2 NPs. NPs: nanoparticles; BA (triangles): assays with biogas A; BAN (circles): assays with biogas A and NPs; BB (diamonds): assays with biogas B; BBN (cross): assays with biogas B and NPs; CACOI: carbon coated zero valent iron.

Table 4
Biomass productivity (Px) and pH of the algal consortium broth supplemented with 10 mg/L of the different nanoparticles. CACOI: carbon coated zero valent iron.

	Fe_2O_3		CACOI		SiO_2	
	Control	10 mg/L	Control	10 mg/L	Control	10 mg/L
P_x (g/L·d)	0.78 ± 0.005	0.87 ± 0.07	1.30 ± 0.07	1.29 ± 0.032	1.32 ± 0.03	1.38 ± 0.06
$pH_{initial}$	7.65 ± 0.04	7.74 ± 0.02	7.86 ± 0.03	7.89 ± 0.01	7.76 ± 0.02	7.70 ± 0.04
pH_{final}	8.85 ± 0.05	8.89 ± 0.10	9.33 ± 0.13	9.28 ± 0.04	9.23 ± 0.10	9.13 ± 0.06

synthesized Fe_2O_3 NPs exhibited an average particle size of 24 nm, which are in the range reported by [33]. Moreover, the morphology of the Fe_2O_3 NPs herein synthesized resulted in a higher BET surface area, which could eventually support a high CO_2 adsorption from biogas. On the other hand, the CACOI NPs presented slightly lower pore volume (0.28 cm^3/g), surface area (27.30 m^2/g) and average pore diameter (41.50 nm), than the Fe_2O_3 NPs, suggesting that both Fe_2O_3 and CACOI NPs can behave similarly as adsorbents. Finally, the SiO_2 NPs presented the highest BET surface area, pore volume and average pore diameter. The values obtained in our particular study ranged between the results reported by [34,35], suggesting that SiO_2 NPs could support superior adsorption properties than CACOI and Fe_2O_3 NPs. Thus, the results of the adsorption/desorption analysis confirmed that nanopowders exhibited a high surface area [36], but the nature of the CACOI and Fe_2O_3 NPs, inherently containing essential trace metals for microalgae growth, could play a key role in microalgae metabolism.

3.2. Influence of type of biogas and nanoparticle addition on microalgae growth

The CO_2 consumption and O_2 production recorded in the headspace of the bottles served as indicators of microalgae growth, along with the optical density of the culture broth (Fig. 2). The addition of biogas B resulted in microalgae inhibition regardless of the presence of NPs, and can be mainly attributed to the absence of sulfur-oxidizing bacteria responsible for the rapid oxidation of H_2S to SO_4^{2-} [37].

On the other hand, biogas A did not induce microalgae inhibition likely due to the absence of H_2S. The cultures containing Fe_2O_3 NPs and SiO_2 NPs exhibited similar cumulative O_2 productions, CO_2 consumptions and culture densities than their controls (in the absence of NPs). Interestingly, Fe_2O_3 NPs have been previously reported as microalgal photosynthesis stimulants, resulting in enhancement in biomass growth and lipid/carbohydrate contents [38]. In our particular study, the addition of 10 mg/L of Fe_2O_3 NPs did not support any significant improvement in CO_2 cumulative consumptions but a slight enhancement of 5 % in O_2 production was observed.

The addition of NPs at 10 mg/L did not enhance Px under biogas A atmosphere in any of the conditions tested. This can be attributed to the microalgae species used in this study, since the effect of the NPs is species specific (Table 4) [8]. Nonetheless, the microalgae cultivated with Fe_2O_3 NPs presented a statistically higher OD_{750}, likely supported by slightly higher O_2 production compared to the control tests. Indeed, the addition of 10 mg/L of Fe_2O_3 NPs stimulated the production of microalgal-bacterial biomass, which is in accordance with [38]. At this point it is important to mention that Xia et al. [38] observed higher biomass growth enhancements at higher Fe_2O_3 NPs concentrations (50 mg/L), which suggested that the concentrations herein assessed were too low, and higher concentrations of Fe_2O_3 NPs can be added to observe an effect on photosynthetic biogas upgrading. Moreover, despite the addition of CACOI NPs resulted in a lower final OD_{750} at the end of the experiment, the reduced lag phase in terms of O_2 production, CO_2 consumption and biomass growth suggested that CACOI NPs stimulated the activity of the algal consortium herein used. Even if little is known about the effect of CACOI NPs on microalgae, our results suggest that these particular NPs do not represent a threat for microalgae growth. Finally, the addition of 10 mg/L SiO_2 under a biogas A atmosphere did not support any statistical difference in the monitored parameters compared to the control tests. SiO_2 NPs were previously reported as stimulants of *Chlorella vulgaris* metabolism, and final dry cell weight of 1.33 g/L were recorded by the addition of SiO_2 NPs [14]. Moreover, the same authors also observed that fatty acid methyl esters productivity was increased up to 0.62 g/L/day by the addition of the SiO_2 NPs. However, in our study no significant change was observed neither in the final dry weight nor in Px by the addition of SiO_2 NPs, probably because the study of Jeon et al. [14] used a concentration of 0.2 wt% SiO_2 NPs, which is much higher than the concentrations herein used. Thus, the absence of impact of SiO_2 NPs on algal metabolism compared to literature can be explained by the significant lower concentration herein used.

Table 5
Biomass productivity (Px) as a function of the type of nanoparticles and light source, at different concentrations. CACOI: carbon coated zero valent iron.

	Fe_2O_3		CACOI		SiO_2	
	Visible light	Visible + UV light	Visible light	Visible + UV light	Visible light	Visible + UV light
Control	1.98 ± 0.30	0.94 ± 0.06	1.24 ± 0.07	2.04 ± 0.10	1.68 ± 0.24	0.90 ± 0.07
20 mg/L	1.44 ± 0.18	1.45 ± 0.13	1.69 ± 0.48	2.00 ± 0.14	1.89 ± 0.08	0.88 ± 0.05
40 mg/L	2.63 ± 0.14	1.41 ± 0.09	2.25 ± 0.55	1.92 ± 0.06	1.89 ± 0.08	0.86 ± 0.05
70 mg/L	2.75 ± 0.23	1.48 ± 0.15	3.12 ± 0.65	2.14 ± 0.03	1.81 ± 0.13	0.85 ± 0.08

CACOI NPs are covered with carbon, and this particular material has been widely used for CO_2 capture [9]. The mechanism of interaction between the NPs and the CO_2 capture is not well understood yet, but one of the main mechanism of interaction is the "shuttle effect", which can be described as follows: CO_2 is adsorbed by the NPs and then the loaded NPs release the adsorbed CO_2 into the aqueous medium, or the algal broth in this case [39]. Thus, the reduced lag phase achieved in the presence of CACOI NPs could be explained by the adsorption capacity of activated carbon [31]. Hence, the CO_2 present in the biogas atmosphere was adsorbed to the surface of the NPs and rapidly released in the aqueous broth for microalgae consumption, thus stimulating an early algal metabolism.

3.3. Influence of nanoparticle concentration under visible light

The addition of 20, 40 and 70 mg/L of Fe_2O_3 NPs resulted in higher cumulative CO_2 consumption and higher Px during the exponential growth phase (Table 5) (Fig. 3). Indeed, the addition of Fe_2O_3 NPs resulted in up to 38 % Px enhancement. The higher Px values herein obtained can be mainly attributed to: 1) the culture media composition, which is a synthetic centrate supporting high biomass productions due to its rich nutrients content compared to other types of wastewater [40]; 2) the high CO_2 concentration in the headspace of the bottle, which resulted in accelerated microalgae growth; 3) the biostimulant nature of the nanoparticles used and 4) the high photosynthetic active radiation and the high illuminated surface to volume ratio. However, the higher the Fe_2O_3 NPs concentration, the higher the lag phase in the assays (Fig. 3a, d, g). This matched the observations of Bibi and co-workers [17], who reported that concentrations of Fe_2O_3 NPs between 50 and 100 mg/L delayed the exponential growth phase of microalgae. Although the cumulative CO_2 consumption and biomass productivity increased with increasing concentrations of Fe_2O_3 NPs, the cumulative O_2 production decreased as the NPs concentration increased. This

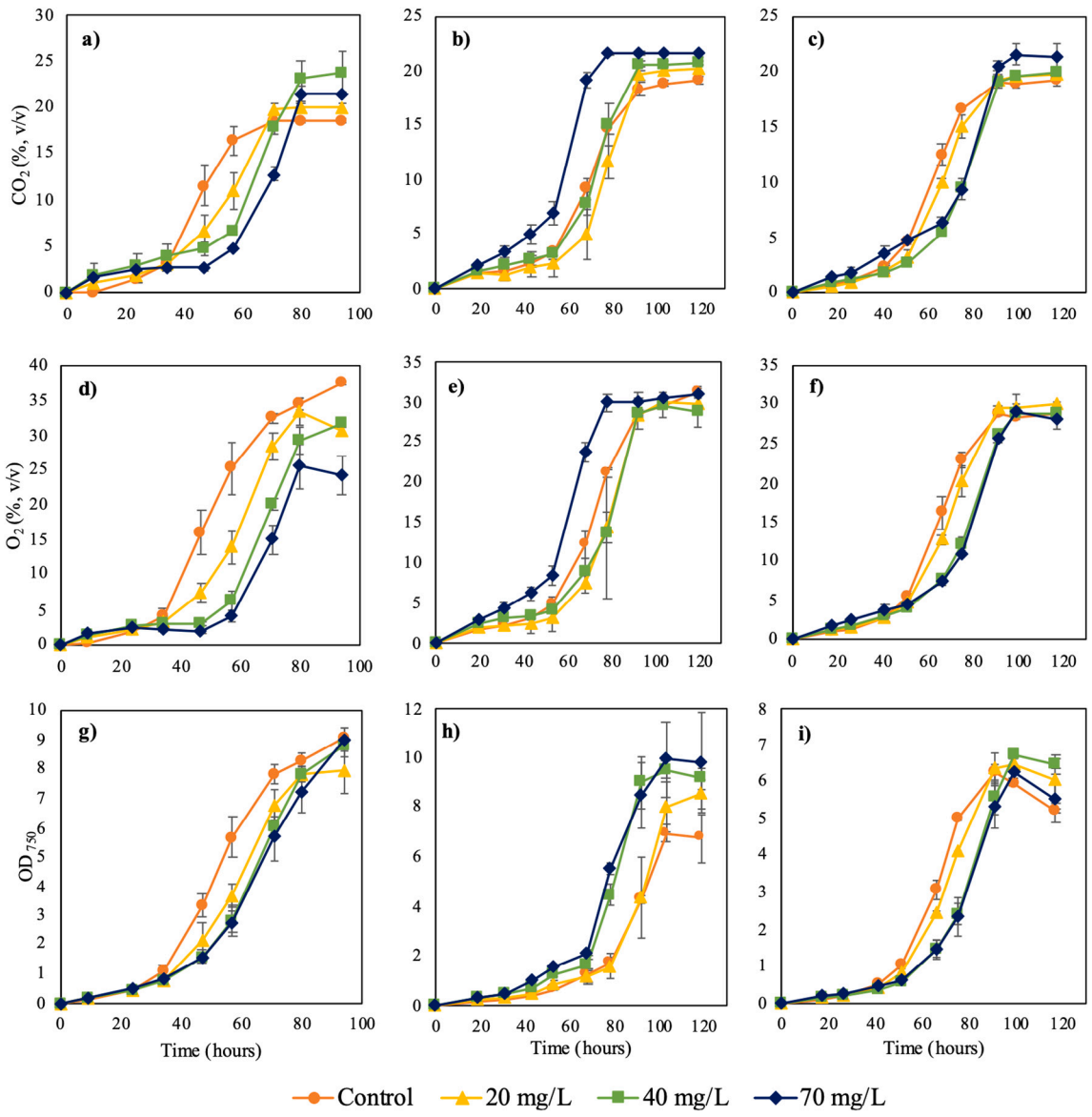

Fig. 3. Time course of the cumulative CO_2 consumption in the assays supplied with different concentrations of a) Fe_2O_3 NPs, b) CACOI NPs, c) SiO_2 NPs; of the cumulative O_2 production in the tests supplemented with different concentrations of d) Fe_2O_3 NPs, e) CACOI NPs, f) SiO_2 NPs; and culture absorbance of the algal consortium supplied with different concentrations of g) Fe_2O_3 NPs, h) CACOI NPs, i) SiO_2 NPs. The assays were run under visible light. CACOI: carbon coated zero valent iron; NPs: nanoparticles.

phenomenon was likely due to the interactions between O_2 and Fe_2O_3 NPs via Fenton reactions, Photo-Fenton reactions, Haber-Weiss reactions or even more complex reactions [41], where the Fe^{2+} ions released by the Fe_2O_3 NPs react with peroxide, water and O_2 to form ROS. Even though the formation of ROS has been considered as one of the major factors that induce toxicity in microalgae [8], the use of Fe_2O_3 NPs presents contradictory results and the tolerance to Fe_2O_3 NPs is species specific. Thus, the retarded exponential phase could be attributed to the presence of ROS. Rana et al. [42] reported that the biomass concentration of *Chlorella pyrenoidosa* was enhanced by 33.7 % when 20 mg/L of Fe_2O_3 NPs were added, which is similar to the biomass enhancements obtained in our study.

The addition of Fe_2O_3 NPs did not enhance the carbohydrates or lipids content of the algal biomass (Fig. 4a) as previously reported by Bibi and co-workers [17]. However, these authors observed that the total lipid content of *C. vulgaris* depends on the time of exposure, and the long term exposure to high Fe_2O_3 NPs concentration resulted in a lipid degradation mediated by a defense mechanism of microalgae against ROS. Thus, the lower lipid content recorded in the assays containing 70 mg/L of Fe_2O_3 NPs is supported by the long term exposure to Fe_2O_3 and to the presence of ROS [17]. Finally, the results herein obtained suggests that Fe_2O_3 NPs acted as CO_2 adsorbents and increased CO_2 availability in the cultivation broth, a phenomenon which has been previously observed in a larger extent at increasing CO_2 concentrations [32]. However, the nature of Fe_2O_3 NPs to Fenton reactions and the formation of ROS interfered in the biomass production and macromolecular accumulation in the microalgae herein used.

Compared to the assays with Fe_2O_3 NPs, the addition of CACOI NPs did not increase the lag phase of algal metabolism. Indeed, the addition of 70 mg/L of CACOI NPs enhanced both Px and the rates of CO_2 consumption, and reduced the lag phase (Fig. 3b, e, h). The cumulative CO_2 consumption in the 70 mg/L CACOI assays was 13 % higher than in the control tests. The latter confirms the fact that CACOI NPs stimulated the CO_2 adsorption mainly by the nature of the material, and the increased CO_2 consumption could be mainly attributed to the higher CO_2 availability in the headspace of the bottles. Notwithstanding, the increasing

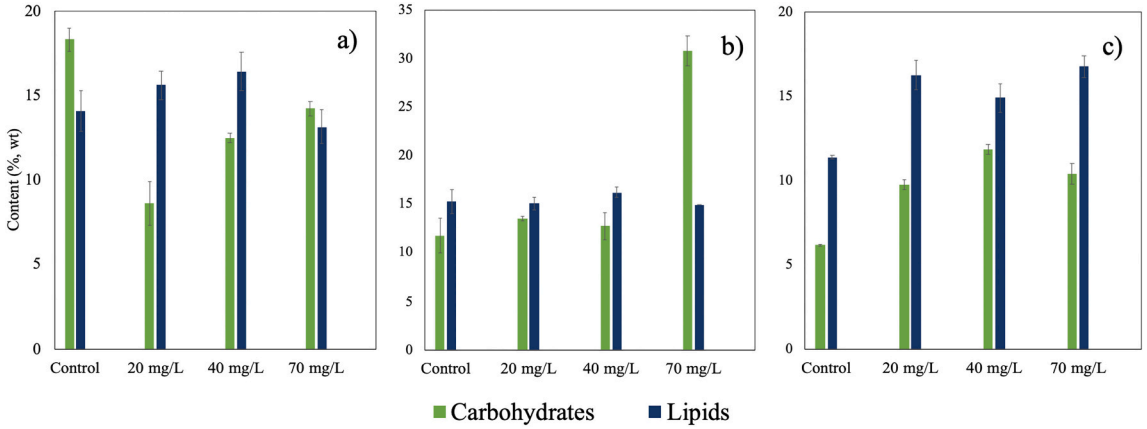

Fig. 4. Influence of the concentration of a) Fe_2O_3 NPs; b) CACOI NPs; c) SiO_2 NPs on the carbohydrate (green) and lipid (blue) content of microalgae biomass at the end of the assays under visible light. CACOI: carbon coated zero valent iron; NPs: nanoparticles. (For interpretation of the references to colour in this figure legend, the reader is referred to the web version of this article.)

concentrations of CACOI NPs did not impact significantly on the cumulative O_2 production and OD_{750}. However the lag phase was significantly increased by the addition of the CACOI NPs, and was related to the increasing concentration. On the other hand, the carbohydrate content of the algal biomass increased by a factor of 2.6 when the cultivation broth was supplemented with 70 mg/L, which can be explained by the superior CO_2 biofixation mediated by the NPs [8]. Thus, the higher CO_2 availability mediated by CACOI NPs at 70 mg/L stimulated the activity of the RuBisCO enzyme, which is widely known to be the catalyst of CO_2 biofixation [13]. Therefore, an enhanced CO_2 biofixation resulted in an increased biomass productivity during the logarithmic growth phase, and in the accumulation of high-value products [13]. Hence, the improved logarithmic phase coupled to the accumulation of carbohydrates confirms that the biofixation capacity of microalgae was significantly improved by the addition of 70 mg/L of CACOI NPs.

Finally, the addition of 70 mg/L of SiO_2 NPs led to a cumulative CO_2 consumption 11.50 % higher than that of the control, thus confirming that SiO_2 NPs acted as CO_2 adsorbents mediating a faster CO_2 dissolution in the algal broth. Notwithstanding, the addition of 40 and 70 mg/L of SiO_2 NPs resulted in a longer lag phase while no statistical difference was observed on the Px. Even if the addition of SiO_2 NPs induced higher cumulative CO_2 consumptions, no statistical difference was observed neither in the cumulative O_2 production nor in OD_{750}, which did not agree with the observations of Jeon and co-workers [14]. The latter confirms the fact that the exposure to NPs is species specific and even if the addition of SiO_2 NPs has been reported to enhanced biomass and lipid production in *C. vulgaris*, the mixed culture used in our study did not experience the same beneficial effects. Interestingly, the addition of SiO_2 NPs enhanced both the carbohydrate and lipid content of the final biomass regardless of the NPs concentration tested. For instance, the addition of 40 mg/L SiO_2 NPs supported the highest carbohydrate content, which was 1.91-fold higher than that in the control assays. Similarly, enhancements in the lipid content ranging by a factor 1.3–1.5 were obtained when SiO_2 NPs were supplemented to the algal broth. Thus, the superior accumulation of carbohydrates and lipids can be explained by the fact that the addition of SiO_2 NPs created a stress environment to the microalgae and, as a response, carbohydrates were accumulated as an energy reserve [43]. On the other hand, lipid accumulation can be explained by the fact that the SiO_2 NPs induced an oxidative stress to microalgae, resulting in a lipid accumulation as a nonenzymatic antioxidant mechanism of defense to scavenge the excessive ROS [44]. Similar findings have been reported by Jeon et al. [14], who reported lipid enhancements of up to 340 % compared to the control mainly attributed to the environmental stress created by the NPs. Thus, our results suggest that the SiO_2 NPs served as CO_2 adsorbents, however the nature of the NPs to created stress conditions that limited the growth of microalgae. Nonetheless, the SiO_2 NPs can be used as a technique to improve the value of the produced biomass.

3.4. Influence of nanoparticle concentration under UV–visible light

Solar UV radiation can seriously affect microalgae integrity and biological function, since it induces the production of ROS [45]. However, Yang et al. [12] recently proved that UV-light mediated a positive effect on CO_2 capture and lipid production in *C. pyrenoidosa* when graphene oxide quantum dots were added. In this context, NPs could act as UV protectors and/or spectrum converters to promote microalgae growth and macromolecule accumulation.

In our study, the addition of Fe_2O_3 NPs supported an enhancement of up to 50 % in Px compared to the control (Table 5). However, no statistical difference was observed in the cumulative CO_2 consumption between the assays (Fig. 5). Furthermore, the cumulative O_2 decreased as the NPs concentration increased. Interestingly, despite the cumulative O_2 concentration was reduced by 30 % at 70 mg/L Fe_2O_3 NPs, the OD_{750} and Px were 26 % and 5 % higher than in the control, respectively. The latter suggests that when Fe_2O_3 NPs were added, the reduction in O_2 content in the headspace did not entail a lower cell growth and this particular behavior can be attributed to the interactions between O_2 and the NPs, which likely caused the formation of ROS. Additionally, the presence of 70 mg/L of Fe_2O_3 NPs resulted in a carbohydrate enhancement of up to 94 % compared to the control assays. However, no statistical difference in term of lipid content was observed among the assays (Fig. 6). Moreover, the supply of UV light in this test series led to a higher lipid production compared to the assays conducted exclusively with visible light regardless of the addition of NPs. Thus, our results are in agreement with the observations of Yang et al. [12], who reported that the addition of graphene quantum dots enhanced the photosynthetic activity and the CO_2 fixation of *C. pyrenoidosa* when exposed to UV-light. Additionally, Dinc et al. [46] has also observed beneficial effects on *C. vulgaris* growth by the addition of Se NPs under UV light, mainly because the NPs scavenge the UV radiation, protecting the microalgal cells. Thus, the Fe_2O_3 NPs herein used stimulated microalgae growth at the highest concentration tested, suggesting that Fe_2O_3 can scavenge the harmful effect of UV radiation resulting in high-value biomass productivity.

On the other hand, despite the increase in CACOI NPs concentration from 20 to 70 mg/L did not enhance Px, the addition of 70 mg/L of NPs resulted in a faster exponential phase and a statistically significant CO_2 consumption enhancement. Interestingly, there was no statistical

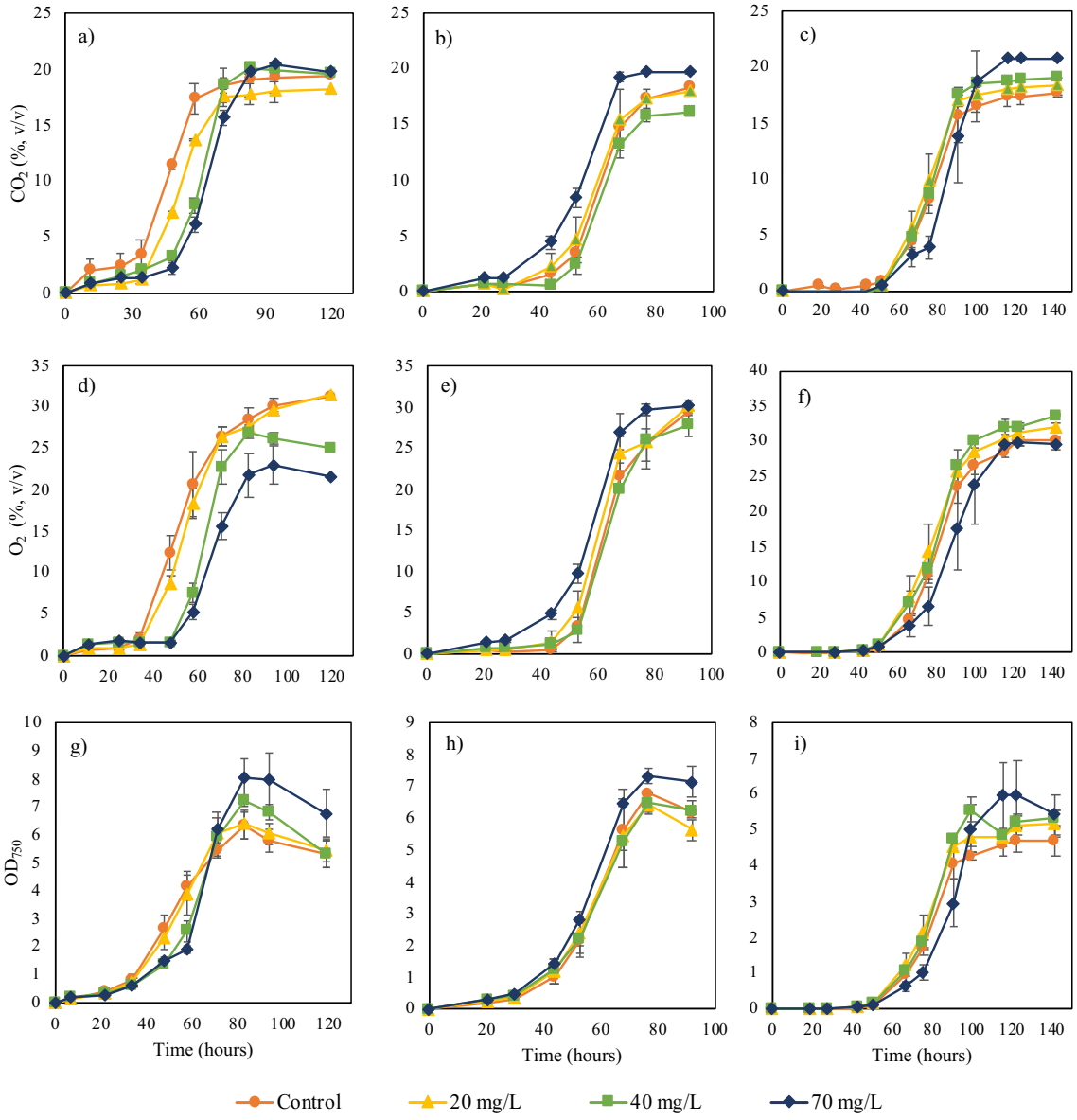

Fig. 5. Time course of the cumulative CO_2 consumption in the assays supplied with different concentrations of a) Fe_2O_3 NPs, b) CACOI NPs, c) SiO_2 NPs; of the cumulative O_2 production in the tests supplemented with different concentrations of d) Fe_2O_3 NPs, e) CACOI NPs, f) SiO_2 NPs; and culture absorbance of the algal consortium supplied with different concentrations of g) Fe_2O_3 NPs, h) CACOI NPs, i) SiO_2 NPs. The assays were run under UV + visible light. CACOI: carbon coated zero valent iron; NPs: nanoparticles.

difference in the cumulative O_2 production between the assays, and the lipid production slightly decreased as the NPs concentration increased. Since this behavior was not observed in the assays carried out only with visible light, the latter suggest that lipid peroxidation in this particular test series was induced by ROS formation mediated by the interaction of the zero valent iron contained in the NPs and the UV light exposure [12]. However, the addition of 70 mg/L induced a carbohydrate content enhancement of up to 22 % and an OD_{750} 15 % higher than the control. The results herein obtained confirm the fact that CACOI NPs effect of microalgae are mainly as CO_2 adsorbents, resulting in enhanced CO_2 availability in the headspace of the bottles. Moreover, the increased CO_2 led to an activation of microalgae metabolism and storage as carbohydrates under both visible and visible + UV light.

Finally, the addition of SiO_2 NPs did not support an enhancement in Px despite the addition of 70 mg/L SiO_2 NPs led to a CO_2 consumption 18 % higher than that recorded in the control tests. Moreover, the addition of 20 and 40 mg/L of SiO_2 NPs led to 11 % and 6 % higher O_2 cumulative productions compared to the control tests, respectively. Additionally, OD_{750} increased as the NPs concentration increased, and the addition of 70 mg/L SiO_2 induced an OD_{750} enhancement of 16 %. Furthermore, the addition of 70 mg/L SiO_2 mediated a 69 % enhancement in the lipid content compared to the control. Finally, our results indicate that the UV-light exposure induce a higher lipid accumulation in microalgae likely due to a mechanism of defense against the generation of ROS [47]. Interestingly, SiO_2 NPs and UV radiation can induce an oxidative stress on microalgae [14]. However, in our particular study, neither biomass loss nor lipid peroxidation by the combination of SiO_2 NPs and UV radiation was observed. Therefore, our results suggest that the oxidative stress caused by SiO_2 NPs did not increase with UV exposure. Thus, even if no biomass enhancements were observed with the addition of SiO_2 NPs neither under visible and visible + UV light exposure, contrary to the observed by Jeon et al. [14], these NPs still can be used as a strategy to produce high-value biomass even under UV radiation.

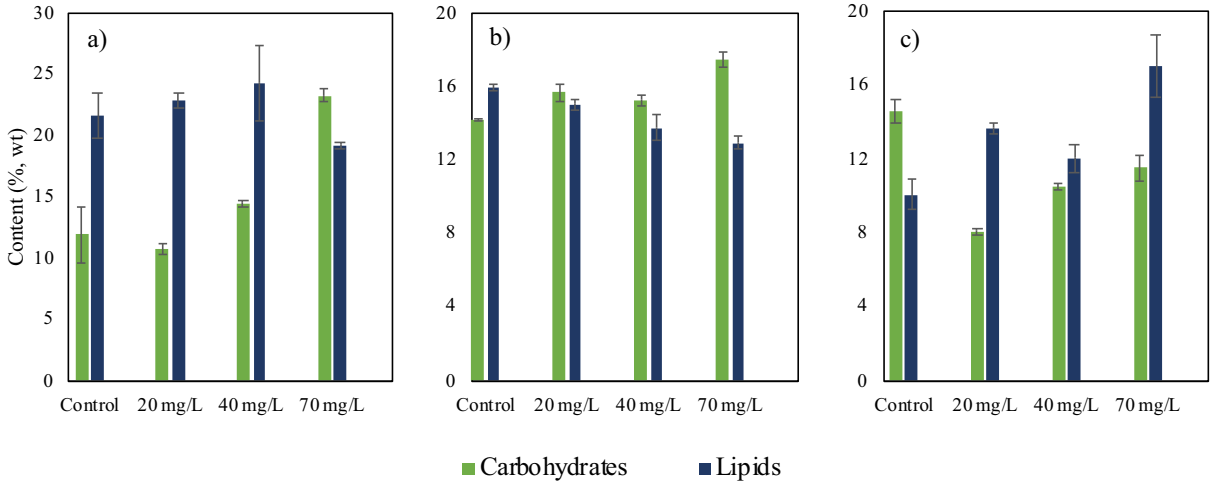

Fig. 6. Influence of the concentration of a) Fe_2O_3 NPs; b) CACOI NPs; c) SiO_2 NPs on the carbohydrate (green) and lipid (blue) content of microalgae biomass at the end of the assays under UV + visible light. CACOI: carbon coated zero valent iron; NPs: nanoparticles. (For interpretation of the references to colour in this figure legend, the reader is referred to the web version of this article.)

4. Conclusions and future prospectives

Fe_2O_3, CACOI and SiO_2 NPs addition to microalgae cultures devoted to biogas upgrading boosted CO_2 adsorption resulting in high-value biomass. Under visible light, the cumulative CO_2 consumptions increased as the NPs concentrations increased. SiO_2 NPs stimulated carbohydrates and lipids production, CACOI NPs supported both increased CO_2 consumptions, higher biomass productivities, shorter lag phases and carbohydrate productions. UV light supply reduced the beneficial effects of NPs, however, the addition of Fe_2O_3 NPs stimulated biomass productivities and carbohydrates, whereas CACOI NPs supported shorter lag phases, increased CO_2 consumption and carbohydrates productions. Finally, the addition of SiO_2 NPs supported lipid production enhancements. Promising results to improve the CO_2 adsorption couple to biomass production and high-value products were obtained in the present study. However, it is important to highlight that these particular results were obtained under controlled conditions. In this regard, future studies should be directed to assess the effect of the NPs on microalgae under uncontrolled conditions, *i.e.* real centrate and environmental conditions. Moreover, life cycle assessments, exergy analyses, techno-economic analyses and energy analyses as described in [48], should be considered to assess the sustainability of the process. Finally, the results herein obtained can be scaled-up to pilot plants to boost CO_2 consumption coupled to microalgae growth. The later could represent a feasible technique to improve the performance of the stablished technology for photosynthetic biogas upgrading.

CRediT authorship contribution statement

Laura Vargas-Estrada: methodology, writing-original draft; Edwin G. Hoyos: methodology, P.J. Sebastian: reviewing, Raúl Muñoz: supervision, reviewing and editing.

Declaration of competing interest

The authors declare that they have no known competing financial interests or personal relationships that could have appeared to influence the work reported in this paper.

Data availability

The data that has been used is confidential.

Acknowledgements

Authors acknowledge CALPECH for providing the CACOI nanoparticles. This work was supported by the Regional Government of Castilla y León and the EU-FEDER (CLU 2017-09, CL-EI-2021-07, UIC 315). Sebastian P.J. acknowledges the financial support from DGAPA-UNAM through the project IN108922. Laura Vargas-Estrada would like to acknowledge CONACYT for her PhD grant.

References

[1] J. Haider, M. Abdul Qyyum, A. Riaz, A. Naquash, B. Kazmi, M. Yasin, A.S. Nizami, M. Byun, M. Lee, H. Lim, State-of-the-art process simulations and techno-economic assessments of ionic liquid-based biogas upgrading techniques: challenges and prospects, Fuel 314 (2022), 123064, https://doi.org/10.1016/j.fuel.2021.123064.
[2] D. Marín, A.A. Carmona-Martínez, S. Blanco, R. Lebrero, R. Muñoz, Innovative operational strategies in photosynthetic biogas upgrading in an outdoors pilot scale algal-bacterial photobioreactor, Chemosphere 264 (2021), https://doi.org/10.1016/j.chemosphere.2020.128470.
[3] E. Mulu, M. M'Arimi, R.C. Ramkat, A. Kiprop, Biogas upgrade using modified natural clay, Energy Convers. Manag. X. 12 (2021), 100134, https://doi.org/10.1016/j.ecmx.2021.100134.
[4] Rodero M. del R., A. Carvajal, Z. Arbib, E. Lara, C. de Prada, R. Lebrero, R. Muñoz, Performance evaluation of a control strategy for photosynthetic biogas upgrading in a semi-industrial scale photobioreactor, Bioresour. Technol. 307 (2020) 123207, https://doi.org/10.1016/j.biortech.2020.123207.
[5] M.del R. Rodero, C.A. Severi, R. Rocher-Rivas, G. Quijano, R. Muñoz, Long-term influence of high alkalinity on the performance of photosynthetic biogas upgrading, Fuel 281 (2020) 118804, https://doi.org/10.1016/j.fuel.2020.118804.
[6] A. Bose, R. O'Shea, R. Lin, J.D. Murphy, A comparative evaluation of design factors on bubble column operation in photosynthetic biogas upgrading, Biofuel Res. J. 8 (2021) 1351–1373, https://doi.org/10.18331/BRJ2021.8.2.2.
[7] A. Bose, R. Lin, K. Rajendran, R. O'Shea, A. Xia, J.D. Murphy, How to optimise photosynthetic biogas upgrading: a perspective on system design and microalgae selection, Biotechnol. Adv. (2019), 107444, https://doi.org/10.1016/J.BIOTECHADV.2019.107444.
[8] L. Vargas-Estrada, A. Longoria, D.M. Arias, P.U. Okoye, P.J. Sebastian, Role of nanoparticles on microalgal cultivation: a review, Fuel 280 (2020), https://doi.org/10.1016/j.fuel.2020.118598.
[9] R. Kumar, R. Mangalapuri, M.H. Ahmadi, D.V.N. Vo, R. Solanki, P. Kumar, The role of nanotechnology on post-combustion CO2 absorption in process industries, Int. J. Low-Carbon Technol. 15 (2020) 361–367, https://doi.org/10.1093/IJLCT/CTAA002.
[10] A. Golmakani, S. Ali Nabavi, B. Wadi, V. Manovic, Advances, challenges, and perspectives of biogas cleaning, upgrading, and utilisation, Fuel 317 (2022), 123085, https://doi.org/10.1016/j.fuel.2021.123085.
[11] E. Mulu, M.M.M. Arimi, R.C. Ramkat, A review of recent developments in application of low cost natural materials in purification and upgrade of biogas, Renew. Sust. Energ. Rev. 145 (2021), 111081, https://doi.org/10.1016/j.rser.2021.111081.
[12] L. Yang, Q. Su, B. Si, Y. Zhang, Y. Zhang, H. Yang, X. Zhou, Enhancing bioenergy production with carbon capture of microalgae by ultraviolet spectrum conversion

via graphene oxide quantum dots, Chem. Eng. J. 429 (2022), 132230, https://doi.org/10.1016/j.cej.2021.132230.
[13] J.Alberto Vieira Costa, M.Greque de Morais, B.da S. Vaz, Physical and biological fixation of CO2 with polymeric nanofibers in outdoor cultivations of Chlorella fusca LEB 111, Int. J. Biol. Macromol. 151 (2020) 1332–1339, https://doi.org/10.1016/j.ijbiomac.2019.10.179.
[14] H.S. Jeon, S.E. Park, B. Ahn, Y.K. Kim, Enhancement of biodiesel production in Chlorella vulgaris cultivation using silica nanoparticles, biotechnol, Bioprocess Eng. 22 (2017) 136–141, https://doi.org/10.1007/s12257-016-0657-8.
[15] E. Kadar, P. Rooks, C. Lakey, D.A. White, The effect of engineered iron nanoparticles on growth and metabolic status of marine microalgae cultures, Sci. Total Environ. 439 (2012) 8–17, https://doi.org/10.1016/J.SCITOTENV.2012.09.010.
[16] K. Pádrová, J. Lukavský, L. Nedbalová, A. Čejková, T. Cajthaml, K. Sigler, M. Vítová, T. Řezanka, Trace concentrations of iron nanoparticles cause overproduction of biomass and lipids during cultivation of cyanobacteria and microalgae, J. Appl. Phycol. 27 (2015) 1443–1451, https://doi.org/10.1007/s10811-014-0477-1.
[17] M. Bibi, X. Zhu, M. Munir, I. Angelidaki, Bioavailability and effect of α-Fe2O3 nanoparticles on growth, fatty acid composition and morphological indices of Chlorella vulgaris, Chemosphere 282 (2021), 131044, https://doi.org/10.1016/j.chemosphere.2021.131044.
[18] H.-Y. Ren, Y.-Q. Dai, F. Kong, D. Xing, L. Zhao, N.-Q. Ren, J. Ma, B.-F. Liu, Enhanced microalgal growth and lipid accumulation by addition of different nanoparticles under xenon lamp illumination, Bioresour. Technol. 297 (2020), 122409, https://doi.org/10.1016/J.BIORTECH.2019.122409.
[19] E. Morelli, E. Gabellieri, A. Bonomini, D. Tognotti, G. Grassi, I. Corsi, TiO2 nanoparticles in seawater: aggregation and interactions with the green alga Dunaliella tertiolecta, Ecotoxicol. Environ. Saf. 148 (2018) 184–193, https://doi.org/10.1016/j.ecoenv.2017.10.024.
[20] S. Manzo, M. Lucia, G. Rametta, S. Buono, G. Di, Toxic effects of ZnO nanoparticles towards marine algae Dunaliella tertiolecta, Sci. Total Environ. 445–446 (2013) 371–376, https://doi.org/10.1016/j.scitotenv.2012.12.051.
[21] C. Zhang, J. Wang, L. Tan, X. Chen, Toxic effects of nano-ZnO on marine microalgae Skeletonema costatum: attention to the accumulation of intracellular zn, Aquat. Toxicol. 178 (2016) 158–164, https://doi.org/10.1016/j.aquatox.2016.07.020.
[22] A. Norouzi, A. Nezamzadeh-Ejhieh, α-Fe2O3/Cu2O heterostructure: brief characterization and kinetic aspect of degradation of methylene blue, Phys. B Condens. Matter 599 (2020), https://doi.org/10.1016/j.physb.2020.412422.
[23] E. Posadas, D. Marín, S. Blanco, R. Lebrero, R. Muñoz, Simultaneous biogas upgrading and centrate treatment in an outdoors pilot scale high rate algal pond, Bioresour. Technol. 232 (2017) 133–141, https://doi.org/10.1016/j.biortech.2017.01.071.
[24] D. Marín, E. Posadas, P. Cano, V. Pérez, S. Blanco, R. Lebrero, R. Muñoz, Seasonal variation of biogas upgrading coupled with digestate treatment in an outdoors pilot scale algal-bacterial photobioreactor, Bioresour. Technol. 263 (2018) 58–66, https://doi.org/10.1016/j.biortech.2018.04.117.
[25] D. Marín, A.A. Carmona-Martínez, R. Lebrero, R. Muñoz, Influence of the diffuser type and liquid-to-biogas ratio on biogas upgrading performance in an outdoor pilot scale high rate algal pond, Fuel 275 (2020), 117999, https://doi.org/10.1016/j.fuel.2020.117999.
[26] E. Posadas, M.L. Serejo, S. Blanco, R. Pérez, P.A. García-Encina, R. Muñoz, Minimization of biomethane oxygen concentration during biogas upgrading in algal–bacterial photobioreactors, Algal Res. 12 (2015) 221–229, https://doi.org/10.1016/J.ALGAL.2015.09.002.
[27] APHA-AWWA-WPCF, Standard Methods for the Examination of Water and Wastewater, 20th ed., 1999, https://doi.org/10.2105/ajph.56.4.684-a. Washington.
[28] M. Dubois, F. Smith, P.A. Rebers, K.A. Gilles, J.K. Hamilton, Colorimetric method for determination of sugars and related substances, Anal. Chem. 28 (1956) 350–356, https://doi.org/10.1021/ac60111a017.
[29] R. Ángeles, E. Arnaiz, J. Gutiérrez, C.A. Sepúlveda-Muñoz, O. Fernández-Ramos, R. Muñoz, R. Lebrero, Optimization of photosynthetic biogas upgrading in closed photobioreactors combined with algal biomass production, J. Water Process Eng. 38 (2020), https://doi.org/10.1016/j.jwpe.2020.101554.
[30] C.D. Powell, A.W. Lounsbury, Z.S. Fishman, C.L. Coonrod, M.J. Gallagher, D. Villagran, J.B. Zimmerman, L.D. Pfefferle, M.S. Wong, Nano-structural effects on hematite (α-Fe2O3) nanoparticle radiofrequency heating, Nano Converg. 8 (2021), https://doi.org/10.1186/s40580-021-00258-7.
[31] M. Munoz, J. Nieto-Sandoval, S. Álvarez-Torrellas, E. Sanz-Santos, B. Calderón, Z. M. de Pedro, M. Larriba, A. Fullana, J. García, J.A. Casas, Carbon-encapsulated iron nanoparticles as reusable adsorbents for micropollutants removal from water, Sep. Purif. Technol. 257 (2021), https://doi.org/10.1016/j.seppur.2020.117974.
[32] A. Hakim, T.S. Marliza, N.M. Abu Tahari, R.W.N. Wan Isahak, R.M. Yusop, W. M. Mohamed Hisham, A.M. Yarmo, Studies on CO2 adsorption and desorption properties from various types of iron oxides (FeO, Fe2O3, and Fe3O4), Ind. Eng. Chem. Res. 55 (2016) 7888–7897, https://doi.org/10.1021/acs.iecr.5b04091.
[33] A. Hakim, T.S. Marliza, M.N. Abu Tahari, M.R. Yusop, M.W. Mohamed Hisham, M. A. Yarmo, Development of α-Fe2O3 as adsorbent and its effect on CO2 capture, Mater. Sci. Forum 840 (2016) 421–426, https://doi.org/10.4028/www.scientific.net/MSF.840.421.
[34] J. Jun Liao, P. Zhao Gao, L. Xu, J. Feng, A study of morphological properties of SiO2 aerogels obtained at different temperatures, J Adv. Ceram. 7 (2018) 307–316, https://doi.org/10.1007/s40145-018-0280-6.
[35] V. Krishnan, J.S. Prakash, V. Manigandan, G.D. Venkatasubbu, A. Pugazhendhi, K. Brindhadevi, T. Kalaivani, Synthesis of mesoporous SiO2 nanoparticles and toxicity assessment in early life stages of zebrafish, Microporous Mesoporous Mater. 330 (2022), 111573, https://doi.org/10.1016/j.micromeso.2021.111573.
[36] V.G. Ilves, A.M. Murzakaev, S.Y. Sokovnin, On the interrelationship of porosity and structural defects in amorphous-crystalline nanopowders SiO2-doped Gd2O3 with their magnetic and luminescent properties, Microporous Mesoporous Mater. 271 (2018) 203–218, https://doi.org/10.1016/j.micromeso.2018.05.044.
[37] M. Franco-Morgado, A. Toledo-Cervantes, A. González-Sánchez, R. Lebrero, R. Muñoz, Integral (VOCs, CO2, mercaptans and H2S) photosynthetic biogas upgrading using innovative biogas and digestate supply strategies, Chem. Eng. J. 354 (2018) 363–369, https://doi.org/10.1016/j.cej.2018.08.026.
[38] C. Xia, Q. Van Le, A. Chinnathambi, S.H. Salmen, S.A. Alharbi, S. Tola, Role of ZnO and Fe2O3 nanoparticle on synthetic saline wastewater on growth, nutrient removal and lipid content of Chlorella vulgaris for sustainable production of biofuel, Fuel 300 (2021), 120924, https://doi.org/10.1016/j.fuel.2021.120924.
[39] I.D. Choi, J.W. Lee, Y.T. Kang, CO2 Capture/Separation control by SiO2 nanoparticles and surfactants, Sep. Sci. Technol. 50 (2015) 772–780, https://doi.org/10.1080/01496395.2014.965257.
[40] X.B. Tan, X.P. Wan, L. Bin Yang, X. Wang, J. Meng, M.J. Jiang, H.J. Pi, Nutrients recycling and biomass production from Chlorella pyrenoidosa culture using anaerobic food processing wastewater in a pilot-scale tubular photobioreactor, Chemosphere 270 (2021), 129459, https://doi.org/10.1016/j.chemosphere.2020.129459.
[41] A. Shokri, M.S. Fard, A critical review in Fenton-like approach for the removal of pollutants in the aqueous environment, Environ. Chall. 7 (2022), 100534, https://doi.org/10.1016/j.envc.2022.100534.
[42] M.S. Rana, S. Bhushan, D.R. Sudhakar, S.K. Prajapati, Effect of iron oxide nanoparticles on growth and biofuel potential of Chlorella spp, Algal Res. 49 (2020), 101942, https://doi.org/10.1016/j.algal.2020.101942.
[43] N. Romero, F.F. Visentini, V.E. Márquez, L.G. Santiago, G.R. Castro, A. M. Gagneten, Physiological and morphological responses of green microalgae Chlorella vulgaris to silver nanoparticles, Environ. Res. 189 (2020), https://doi.org/10.1016/j.envres.2020.109857.
[44] F. Wang, T. Liu, W. Guan, L. Xu, S. Huo, A. Ma, G. Zhuang, N. Terry, Development of a Strategy for Enhancing the Biomass Growth and Lipid Accumulation of Chlorella sp . UJ-3 Using Magnetic Fe 3 O 4 Nanoparticles, 2021.
[45] R.P. Rastogi, D. Madamwar, H. Nakamoto, A. Incharoensakdi, Resilience and self-regulation processes of microalgae under UV radiation stress, J. Photochem. Photobiol. C Photochem. Rev. 43 (2020), 100322, https://doi.org/10.1016/j.jphotochemrev.2019.100322.
[46] S.K. Dinc, O.A. Vural, F.E. Kayhan, N.O. San Keskin, Facile biogenic selenium nanoparticle synthesis, characterization and effects on oxidative stress generated by UV in microalgae, Particuology. 70 (2022) 30–42, https://doi.org/10.1016/j.partic.2021.12.005.
[47] M.K. Nguyen, J.-Y. Moon, V.K.H. Bui, Y.-K. Oh, Y.-C. Lee, Recent advanced applications of nanomaterials in microalgae biorefinery, Algal Res. 41 (2019), 101522, https://doi.org/10.1016/J.ALGAL.2019.101522.
[48] M. Aghbashlo, H. Hosseinzadeh-Bandbafha, H. Shahbeik, M. Tabatabaei, The role of sustainability assessment tools in realizing bioenergy and bioproduct systems, Biofuel Res. J. 9 (2022) 1697–1706, https://doi.org/10.18331/BRJ2022.9.3.5.